

# A new Hamiltonian model of the Fibonacci quasicrystal using non-local interactions: simulations and spectral analysis

Amrik Sen<sup>1a</sup> and Carlos Castro Perelman<sup>2,3b</sup>

<sup>1</sup> School of Mathematics, Thapar Institute, Patiala, Punjab, India.

<sup>2</sup> Centre for Theoretical and Physical Sciences, Clark Atlanta University, Georgia, USA.

<sup>3</sup> Ronin Institute, 127 Haddon Pl. Montclair, NJ 07043, USA.

Received: date / Revised version: date

**Abstract.** This article presents a novel Hamiltonian architecture based on *vertex types* and *empires* for demonstrating the emergence of aperiodic order (quasicrystal growth) in one dimension by a suitable prescription for breaking translation symmetry. At the outset, the paper presents different algorithmic, geometrical, and algebraic methods of constructing empires of vertex configurations of a given quasi-lattice. These empires have *non-local* scope and form the building blocks of the new lattice model. This model is tested via Monte Carlo simulations beginning with randomly arranged  $N$  tiles. The simulations clearly establish the Fibonacci configuration, which is a one dimensional quasicrystal of length  $N$ , as the final relaxed state of the system. The Hamiltonian is promoted to a matrix operator form by performing dyadic tensor products of pairs of interacting empire vectors followed by a summation over all permissible configurations. A spectral analysis of the Hamiltonian matrix is performed and a theoretical method is presented to find the exact solution of the attractor configuration that is given by the Fibonacci chain as predicted by the simulations. Finally, a precise theoretical explanation is provided which shows that the Fibonacci chain is the most probable ground state. The proposed Hamiltonian is a one dimensional model of quasicrystal growth.

**PACS.** 61.44.Br Quasicrystals – 75.10.Hk/Jm Classical/Quantized spin models – 05.50.+q Lattice theory

## 1 Introduction

The simplest geometrical construct for generating a one dimensional quasicrystal, such as the Fibonacci chain, is by the cut and project procedure from a strip embedded in the two dimensional  $\mathbb{Z}_2$  lattice and with a slope proportional to the Galois conjugate  $-\frac{1}{\phi}$ , where  $\phi = \frac{1+\sqrt{5}}{2}$  is the golden mean [1, 2]. The method can be replicated to generate higher dimensional quasi-lattices. However, this purely geometrical construction does not lend a physical picture of the processes that may be involved in the generation of a simple aperiodic lattice. Specifically, it is of immense importance to experimentalists and material scientists to understand the physics of quasicrystal growth [3, 4]. Besides, a physical picture of the emergence of translation asymmetry in crystals may be of general interest to scientists striving to unravel the laws of nature through the study of symmetries and conservation principles [5, 6, 7, 8].

### 1.1 Known models of quasicrystal growth

In 2008, writing under the *Solid-state physics* section of Nature, Paul J. Steinhardt posed a fundamental question: *How does your quasicrystal grow?* [9]. Broadly speaking, theoretical approaches to understand the growth of quasicrystals have been undertaken along two distinct modes of enquiry, viz., rule-based methods [10, 11, 12, 13, 14, 15] and variants of lattice models using molecular dynamics simulations [16, 17, 18, 19]. The lattice models typically have spinorial generators defined by the Pauli spin matrices [20] that form the bases of the special unitary group  $SU(2)$  [21]. The connection between the symmetry of the aforementioned group and the absence of translation symmetry of quasicrystals is not obvious. This presents us with an opportunity to devise an alternative new lattice model for which the connection between the higher dimensional translation symmetry of the generating mother lattice (2D in this case) and the emergent asymmetry of the quasicrystal (aperiodic order) is clear. The present article attempts to address this point. Capturing this relationship with a higher dimensional space in a realistic model of quasicrystal is important because it allows us to study the dynamics of low frequency phason modes [22]. Research on understanding the fundamental structural (atomic) arrange-

<sup>a</sup> amriksen@thapar.edu

<sup>b</sup> perelmanc@hotmail.com

ments in aperiodic lattices is essential because phason degrees of freedom in quasicrystals enable the modeling of complex dynamical processes [23, 24, 25, 26, 27, 28, 29]. Specifically, they allow us to study the dynamics of periodic and quasiperiodic structures with anharmonic interactions both by analytical calculations and by molecular dynamics simulations [30, 31]. Historically, lattice models like the Ising model and its variants have been extensively used to investigate various aspects of phason dynamics and atomic structures pertaining to quasicrystals [32, 33, 34, 35]. With the development of new lattice models, investigation of phason modes of aperiodic systems driven by quasi-periodic potentials [36] can be expanded further. The mechanism by which crystal symmetry is broken manifests in many forms. In a very recent paper, a group of researchers have studied and demonstrated the manner in which quasicrystalline structures can emerge by spontaneous breaking of discrete time translation symmetry of a time-periodic Hamiltonian of a many body system [37]. Signatures of Fibonacci order have also been reported by considering asymmetric Van der Pol-Duffing oscillators in an appropriate parameter space [38].

Many authors have primarily focussed on studying the Ising model with spin interactions prescribed by the Fibonacci quasicrystal [39, 40] and have analyzed spectral behavior of Fibonacci oscillators by considering Ising like models with atoms spaced according to the Fibonacci chain [41]. Additionally, several authors have studied electronic structures and energy spectrum of Fibonacci quasicrystals by considering tight binding Hamiltonian models with hopping constants prescribed by a finite Fibonacci word (Fibonacci approximant) [43, 45, 44, 42, 46]. There is an apparent dearth of lattice models whose ground state is the Fibonacci configuration. Such models may be a better candidate for experimental explorations. Unlike the aforementioned investigations, the current work addresses this gap and presents a lattice Hamiltonian whose ground state is the Fibonacci state with the highest probability and therefore is a *physical* model for explaining the manner in which quasicrystals grow purely based on energetics. This will open new research avenues for studying properties of quasicrystals using techniques cited above in this section based on the Hamiltonian model presented in this article.

## 1.2 Scope of this work

This research paper presents a new Hamiltonian architecture using *vertex configurations* (VCs) and their respective *empires* to understand the nature of atomic rearrangements compatible with the emergence and growth of quasicrystals in one dimension. This formulation has the advantage of encoding non-local interactions directly through the non-local scope of empires of the VCs, i.e. locality is neither assumed a priori for any interaction (like in the case of the nearest neighbor Ising model) nor is it erroneously concocted to serve as a precursor to any emergent non-locality. The proposed Hamiltonian architecture is a first principles approach belonging to a class of integrable lattice models and at the same time, is formulated

in terms of matrix operators that have a clear geometric interpretation. The simulations of the proposed Hamiltonian model demonstrate the manner in which a random assortment of tiles, self interact and rearrange to form a one dimensional Fibonacci quasicrystal. A detailed spectral analysis of the Hamiltonian operator reveals that the Fibonacci state is the most likely ground state of the system. This aperiodic Fibonacci ground state can be generated entirely by the interaction of a collection of sub-states (empires) of different chain configurations undergoing energetic relaxation. This paper presents a new physical model of quasicrystal growth in one dimension.

## 1.3 Organization of this paper

Section 2 introduces the definition of Fibonacci words in a recursive manner, and presents three different methods of constructing empires for a given VC in a Fibonacci chain. While the geometric method is primarily useful for implementing the Monte Carlo simulations discussed in the latter section, the algebraic expression of the empires of a Fibonacci chain will be key to understand the manner in which the translation symmetry is broken as discussed later. Section 3 discusses the implementation of the Monte Carlo simulation of the new Hamiltonian model and presents results of these simulations. Section 4 presents the operator form of the Hamiltonian and discusses the construction of the matrix algebra. In this section, spectral analysis of the Hamiltonian operator is presented and these analytical results are compared with the results of the simulations. A direct physical explanation is provided as to why the Fibonacci chain is the most likely ground state of the system as is evident from the simulations. In sections 5 and 6, a summary of the main contributions of this paper is presented and future plans to extend the work to two dimensional quasicrystals are outlined.

At the very outset, it must be carefully noted that unless otherwise specified, by the phrase *Fibonacci chain*, we refer to the finite Fibonacci approximant in this article. This terminology is interchangeably used with equivalent phrases such as *Fibonacci configuration* and *Fibonacci state*.

## 2 The Fibonacci lattice

A Fibonacci sequence is constructed from the Fibonacci numbers by using the following recurrence relation,

$$F_{n+1} = F_n + F_{n-1}, \quad (1)$$

where  $F_0 = 0, F_1 = 1$ . An interesting property of this sequence is the golden ratio scaling,  $\lim_{n \rightarrow \infty} \frac{F_{n+1}}{F_n} = \phi$  where the rapid convergence to  $\phi$  (the golden ratio) can be verified in a simple manner [47]. A Fibonacci word is constructed using the following recurrence relation,

$$S_n = S_{n-1}S_{n-2}, \quad n \geq 2, \quad (2)$$

with  $S_0 = 0, S_1 = 01$ . Thus a Fibonacci word of length  $n$  is a finite sequence of 0 and 1 constructed as above [48, 49]. The relationship between a finite Fibonacci word and the Fibonacci sequence stems from the fact that the length of  $S_n$  is  $F_{n+2}$ , the  $(n+2)^{\text{th}}$  Fibonacci number. A Fibonacci lattice or Fibonacci quasicrystal of size  $n$  is a lattice with grid spacing encoded by the Fibonacci word  $S_n$  where  $0 \rightarrow \phi$  and  $1 \rightarrow 1$ . A standard representation of such a quasi lattice is given by replacing 0 by  $L$  and 1 by  $S$  where the symbols  $L$  and  $S$  are regarded as *tiles*. Eg., a section of a Fibonacci quasicrystal in the  $L, S$  representation looks like  $\dots L S L L S L S L L L S \dots$ . Thus, a Fibonacci lattice is a quintessential example of a one dimensional quasicrystal.

## 2.1 Vertex configurations and empires

The model demonstrated in this manuscript is designed based on VCs and empires. These are standard canonical descriptors of quasicrystals [50]. For the 1D Fibonacci quasicrystal, there are three VCs, viz.,  $\{L, L\}, \{L, S\}, \{S, L\}$ . Note that the tile  $S$  cannot appear in succession in a Fibonacci lattice and hence  $\{S, S\}$  is not a legal VC.

### 2.1.1 Notations and definitions

**Empire:** Corresponding to each vertex type (vertex configuration) at each coordinate, there is a set of *forced* tiles that constitute the respective empire [51, 52, 53, 54, 55, 56]. The precise formulation of an empire for a given VC will become clear through the detailed discussions of this section.

Generally speaking, there are three ways of constructing empires of a VC in a quasicrystal. For the one dimensional case, a simple substitution rule may be used to enlist the empires for any vertex configuration [2]. Alternatively, a geometric method using an irrational projection from a two dimensional lattice may be used to generate the empires of a given VC [57, 58]. Finally, a new set of algebraic formulae for the empires of the one dimensional Fibonacci quasicrystal is developed for the first time to our knowledge and presented here. All these methods are discussed in an elaborate manner in the context of the one dimensional Fibonacci quasicrystal.

In what follows, the mathematical notation and definitions of the related terms are given below.

---


$$\begin{aligned}
 V : & \quad \text{set of VCs (vertex configurations)} = \{\{L, L\}, \{L, S\}, \{S, L\}\} \\
 X : & \quad \text{set of coordinates denoted by subscript numerals, i.e. } (x_0, x_1, x_2, \dots) \equiv (0, 1, 2, \dots) \\
 \alpha_j : & \quad \text{the VC } \alpha \text{ located at coordinate } j \\
 E_{\alpha_j, l} = & \quad \begin{cases} +1, & \text{if tile located at } l \text{ is } S \\ -1, & \text{if tile located at } l \text{ is } L \\ 0, & \text{otherwise (i.e. unforced tile).} \end{cases} \\
 \tau_i : & \quad \text{binary representation of the tiling space with entries 1 for } S \text{ and } -1 \text{ for } L. \\
 \Omega : & \quad \text{domain of the lattice containing the set } \{\alpha_i\}_{i=2:N} \text{ where } N \text{ is the length of the lattice.}
 \end{aligned} \tag{3}$$


---

For the sake of notational brevity, a tile referenced by the coordinate  $l$  means that the tile is located between the lattice coordinates  $l$  and  $l+1$  for a right sided entry and between the coordinates  $-l$  and  $-l-1$  for a left sided entry. For example, consider the chain expressed by (5). The tile referenced by  $l=1$  is  $S$  located between  $l=1$  and  $l+1=2$ .<sup>1</sup> A VC referenced by coordinate  $j$  refers to the one composed of the tiles on either side of  $j$ . Finally, the VC-empire parameterization encompasses the local and non-local *field of influence* of a given VC through its domain of influence by the forced tiles. Concisely, this empire *field* of VC  $\alpha$  situated at  $j$  is denoted by the empire vector

$$\mathbf{E}_{\alpha_j} = (\dots E_{j,-2}^{\alpha L} E_{j,-1}^{\alpha L} E_{j,0}^{\alpha L} E_{j,0}^{\alpha R} E_{j,1}^{\alpha R} E_{j,2}^{\alpha R} \dots),$$

<sup>1</sup> Left and right sided entries in an empire vector are with reference to the coordinate located at the center of the VC, this is analogous to a *radial* convention with the center of the VC as the origin.

where superscripts  $L$  and  $R$  refer to left and right sided entries respectively. In the following three sections, we discuss three different methods of finding the empires of VCs. The substitution method and the geometric method of constructing empires have been explored by others in the past but the algebraic prescriptions of the empires are new results presented here.

### 2.1.2 Substitution algorithm for constructing empires

This algorithm borrows extensively from detailed discussions on substitution rules for generating aperiodic Fibonacci words in ch. 4 of the text by Baake and Grimm [2]. This method is applicable for the one dimensional Fibonacci chain but may be extended as a principle to a network of Fibonacci chains. The identification of the empire tiles in a real Fibonacci chain, denoted by uppercase





prepending 1 to the Fibonacci word defined by the recursion (2),  $f_1 = 0$ ,  $f_2 = 1$ , etc..  $\lfloor \cdot \rfloor$  is the standard *floor* operator that outputs the integer part of the argument. For consistency, entries from eq. (9) are compared with that of entries from eq. (7).  $E_{0,0}^{1R} = -1$ ,  $E_{0,1}^{1R} = 1(0+1) - 0 = 1$ ,  $E_{0,2}^{1R} = 0(1+0) - 1 = -1$ ,  $E_{0,3}^{1R} = 0(0+1) - 0 = 0$ ,  $E_{0,4}^{1R} = 1(0+0) - 0 = 0$ ,  $E_{0,5}^{1R} = 0(1+0) - 1 = -1$ .

Owing to the symmetry of the  $\{L, L\}$  VC, using  $f_{-n} = f_n$  in conjunction with the formula given by eq. (9), gives the entries of the empire vector to the left of  $\mathbf{LL}$ . For a symmetric VC like  $\{L, L\}$ , the following is trivially true:  $E_{-n}^{1L} = E_n^{1R}$ . Here  $L$  corresponds to left and the convention for referencing the tiles is the following:

- tiles to the right of the VC are referenced by the coordinate  $x_l$  to their immediate left, and
- tiles to the left of the VC are referenced by the coordinate  $x_l$  to their immediate right,

i.e. the convention follows a radial indexing scheme with the center of the VC located at  $x_j$  ( $x_0$  in the above example) as the origin. Additionally,  $E_{0,0}^{1R} = E_{0,0}^{1L}$ , each referencing the right and left tiles that respectively constitute the VC. Finally,  $\mathbf{E}_j^1 = \mathbf{E}_j^{1L} + \mathbf{E}_j^{1R}$  constitutes the full empire vector. Here

$$\mathbf{E}_{j=0}^{1L} = (\dots E_{0,-5}^{1L} E_{0,-4}^{1L} E_{0,-3}^{1L} E_{0,-2}^{1L} E_{0,-1}^{1L} E_{0,0}^{1L} 0 0 0 0 0 \dots)$$

and likewise for  $\mathbf{E}_{j=0}^{1R}$ . For brevity, the superscripts  $L$  and  $R$  are often omitted and the sign of the subscript  $n = l - j$  is sufficient to identify the left and right tiles.

**Asymmetric VC,  $\{L, S\}, \{S, L\}$ :** Similarly, exact formulations of the asymmetric VCs are given below for the first time to our knowledge.

$$E_n^{3R} = \begin{cases} -1; & n = 0 \\ 3 + u_n - u_{n+2}; & n \geq 1, \end{cases} \quad E_n^{2R} = \begin{cases} 1; & n = 0 \\ -1; & n = 1 \\ E_{n-1}^{3R}; & n > 1. \end{cases} \quad (10)$$

By symmetry, the left sided entries are

$$E_{-n}^{3L} = E_n^{2R}, \quad n \geq 0 \\ E_{-n}^{2L} = E_n^{3R}, \quad n \geq 0. \quad (11)$$

Clearly, the non-trivial empire tiles obey the following relations  $E_{-n}^3 = E_n^2$ ,  $E_{-n}^2 = E_n^3$ ,  $n > 0$ . Moreover,  $\mathbf{E}_j^\alpha = \mathbf{E}_j^{\alpha L} + \mathbf{E}_j^{\alpha R}$  constitutes the full empire vector for the VCs  $\alpha = 2, 3$ . The definitions of  $u_n$ ,  $\mathbf{E}_j^{\alpha L}$  and  $\mathbf{E}_j^{\alpha R}$  are as described earlier. Note that for an asymmetric VC, the  $0^{th}$  mode empire tiles  $\mathbf{E}_{0,0}^{\alpha L} \neq \mathbf{E}_{0,0}^{\alpha R}$  are defined as above.<sup>3</sup> This completes the parametrization of the 1D Fibonacci chain in terms of the VCs and the corresponding empires.

<sup>3</sup> The trivial empire tiles correspond to the tiles of the VC only.

## 2.2 Random flips

The Monte Carlo simulations of section 3 below employ random flips to span the different chain configurations. A random flip can be categorized as follows:

1. **symmetric flip:** For the 1D case, this refers to the flips of the type  $\{L, S\} \leftrightarrow \{S, L\}$ . A flip of this kind preserves the local length at the location of the flip.
2. **asymmetric flip:** This refers to the flips of the type  $\{L, L\} \leftrightarrow \{S, L\}$  or  $\{S, L\} \leftrightarrow \{L, L\}$ , etc. A flip of this kind does not preserve the length of the quasicrystal section locally and results in a defect and must be accompanied by a simultaneous flip (possibly near the original flip) of a similar kind so that the total length of the section within the two flips is conserved.

## 3 Hamiltonian

The canonical Hamiltonian  $H_\Omega$  for the 1D Fibonacci system is constructed as follows:

$$H_\Omega = -\frac{1}{N} \underbrace{\sum_{k,i \in X} B_{k,i} E_{\alpha_k, i}}_{\text{interaction free terms}} - \frac{1}{N} \underbrace{\sum_{j,i \in X} J_{j,i} \langle \mathbf{E}_{\alpha_j} | \mathbf{E}_{\alpha_i} \rangle}_{\text{interaction terms}} \equiv -\frac{1}{N} B_{k,i} E_{\alpha_k, i} - \underbrace{\frac{1}{N} J_{j,i} \langle \mathbf{E}_{\alpha_j} | \mathbf{E}_{\alpha_i} \rangle}_{\text{Einstein summation notation}}, \quad (12)$$

where  $B_{k,i}$  and  $J_{j,i}$  are the free parameters of the model with units of energy and  $\mathbf{E}_{\alpha_j} \equiv \mathbf{E}_j^\alpha$  is a dimensionless vector of 0s and  $\pm 1$ s denoting the empire of the VC  $\alpha$  located at  $j$ . Here,  $\langle \cdot | \cdot \rangle$  denotes an inner product operation:  $\langle \mathbf{A} | \mathbf{B} \rangle := \sum_i A_i B_i$ , where  $\mathbf{A}, \mathbf{B}$  are vectors with entries  $A_i$  and  $B_i$  respectively. The locations of the forced tiles are referenced by the elements  $\pm 1$  in the vector  $\mathbf{E}_{\alpha_j}$  depending on whether the forced tile in question is  $S$  or  $L$ . The Hamiltonian in eq. (12) has two terms, viz., the inter-

action free term which expresses the energy of a given VC (in conjunction with its empire field) in an external field or in vacuum, and the interaction term that encompasses the mutual energy of interaction of two distinct VCs through the interaction of their respective empires. It is important to note that by construction, the empire interactions are non-local because the values of  $m$  and  $n$  can be far apart.

### 3.1 Metropolis-Hastings simulation of the Hamiltonian

The algorithm first chooses selection probabilities  $p_s(\mu, \nu)$  which represent the probability that state  $\nu$  is selected by the algorithm out of all states given that the previous state is  $\mu$ . It then uses acceptance probabilities  $p_a(\mu, \nu)$  that ensure the detailed balance condition. This is a class of molecular dynamics simulation that is generally used to study lattice models [18, 30].

#### 3.1.1 Simulation steps

1. A lattice site is randomly picked from the Fibonacci grid using selection probability  $p_s(\mu, \nu)$  and the contribution to the total energy involving the VC at this site is calculated.
2. The VC is flipped and the new contribution to the energy is calculated. The flip may be  $LL \rightarrow LS, LS \rightarrow SL, SL \rightarrow LL$ , etc.
3. If the new energy is less, then the flipped value is retained.
4. If the new energy is more, then the flipped value is retained with probability  $e^{-\beta(H_\nu - H_\mu)}$ . Here  $\beta = \frac{1}{k_B T}$  where  $k_B$  is the Boltzmann's constant and  $T$  is the temperature. For the simulations reported here,  $T$  is suitably set to  $0.6K$  to allow for an orderly final configuration of the chain.
5. The process is repeated until a global minimum of the total energy is attained.

The interaction mechanism in this case involves the empire of the flipped VC with the empires of all other (non flipped) VCs. This scenario is reminiscent of a spontaneous (empire) field interaction due to an impulse perturbation (single flip) with the background empire field (owing to the existing non-flipped VCs and their empires). This algorithm can be extended to more than two simultaneous flips. The interaction mechanism in this case involves the empire of each of the flipped VCs with the background empire field (due to the non-flipped VCs) in conjunction with an interfering competition between the flipped VCs and their empires. In this case, either the ripples created by both the flips get annihilated by the background field or the ripples caused by one of the flips annihilate those of the other field. In any case, the simplest strategy as illustrated by the algorithm mentioned above is considered here.

### 3.2 Results of simulations of one dimensional quasicrystal growth

Several simulation runs with chains of different lengths ( $N = 5, 8, 13, 21, 34, 55, 89, 144$ , and  $233$ ) were performed starting with different initial states of the chain. In each case, the attractor, that minimized the total Hamiltonian, was found to be the Fibonacci chain. In Figures 2 and 3, an example of one such simulation with  $N = 34$  is presented.

A selected number of movies of the simulations can be found in the first author's youtube channel.<sup>4</sup>

### 3.3 Distribution of the attractor and invariance of the Hamiltonian to initial conditions

It is important to note that by establishing the Fibonacci chain (a.k.a. the Fibonacci state) as the attractor of the Hamiltonian (12), as shown by the simulations, we are essentially interested in the relative distribution of the  $L$  and  $S$  tiles. In the next section, we invoke the ansatz that the distribution of the sign of the entries of the most relevant eigenvector of the Hamiltonian matrix prescribes the attractor configuration. The applicability of this ansatz is found to be consistent by treating the Hamiltonian as a quantum mechanical system and verifying one of the main axioms of probability as discussed in the subsequent section. It must be noted that the choice of labels for the ternary system used in the definition of the empires in section 2.1 is entirely arbitrary and a matter of computational convenience. It must be emphasized that the results of the simulations are invariant to the initial state of the chain as is shown by the above cited movies of the simulations and Figures 2 and 3.

## 4 Empire dyads, spectral analysis, and the Fibonacci state

In order to formulate an algebraic representation of the Fibonacci system and the associated empire dyads, it is essential to promote the Hamiltonian defined by eq. 12 to a matrix operator form. Moreover, since the external field  $B_{\alpha_k, i}$ , plays no influence on the final attractor configuration, the interaction free term will be omitted from consideration in the theoretical analysis of the Hamiltonian presented in this section. This is a matter of convenience without any loss of generality. More importantly, the absence of the external field  $B \equiv 0$  will allow us to invoke postulates of quantum mechanics to analyze the classical lattice model (12). This is similar in spirit to the direct correspondence between the quantum Ising model and the classical Ising model in the absence of external magnetic field [20, 59, 60].

### 4.1 Construction of empire dyads and the Hamiltonian matrix operator

Consider any chain (not necessarily Fibonacci) of fixed length  $N$  (i.e.  $N$  lattice sites) where  $N$  is moderately large. The matrix operator, corresponding to a pair of interacting empire vectors<sup>5</sup> of VCs  $\alpha$  and  $\beta$  located at positions

<sup>4</sup> <https://www.youtube.com/watch?v=MirQPchbo7Q>

<https://www.youtube.com/watch?v=1n-je95j01k>

[https://www.youtube.com/watch?v=\\_KsTo0Qs5hc](https://www.youtube.com/watch?v=_KsTo0Qs5hc)

<sup>5</sup> Note that the geometric method of constructing empires enables us to find the empire of a VC located at a certain

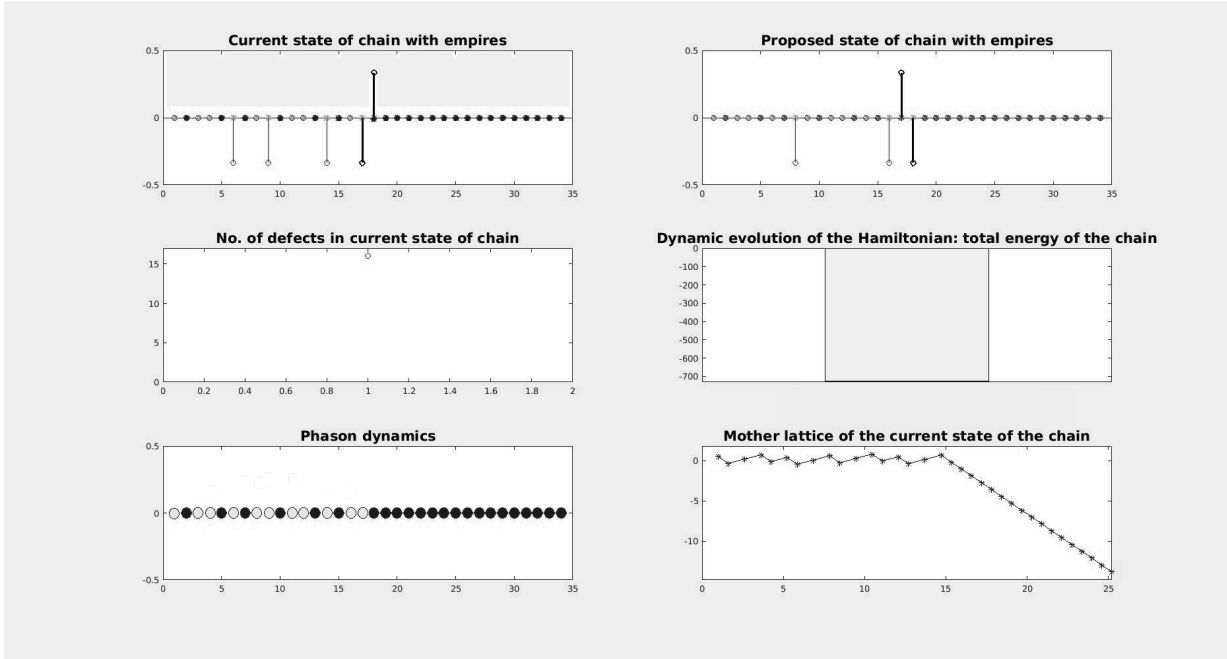


Fig. 2: The set of plots corresponds to the initial state of the chain (bottom left panel) at the start of the simulation where the tiles  $L$  and  $S$  are color coded as light and dark respectively. The VC pairs being flipped are shown by the black colored stem pairs displayed in the top panels. The number of defects in the current state of the chain corresponds to the number of forbidden elementary configurations ( $LLL$  and  $SS$ ) in a Fibonacci chain. The coordinates of the 2D lattice (mother lattice, ref. Figure 1), from which the current state of the chain may be constructed, are shown in the bottom right panel. The total Hamiltonian ( $NH_{\Omega}$ ) of the current configuration is displayed in the middle right panel.

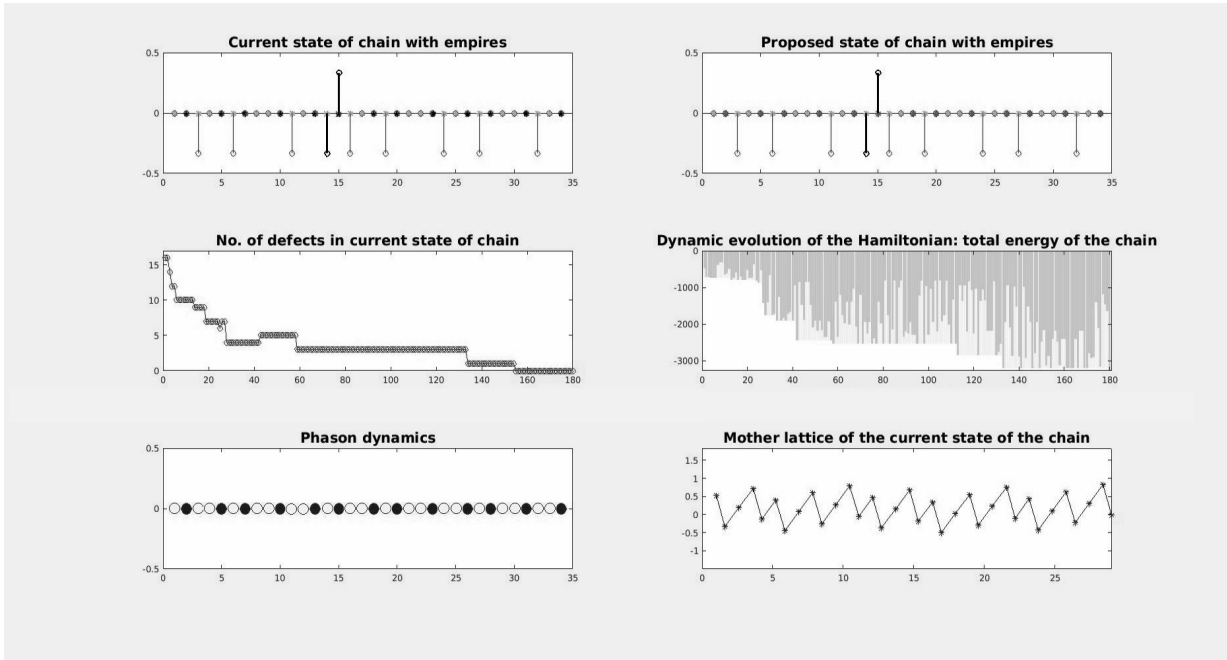


Fig. 3: The set of plots here corresponds to the final relaxed state of the chain. The arrangement of the light ( $L$ ) and dark ( $S$ ) balls clearly shows that the attractor configuration is the Fibonacci chain. The evolution of the total Hamiltonian ( $NH_{\Omega}$ ) of the system is also displayed clearly demonstrating that the attractor configuration has the minimum energy. The defect counter shows the absence of any forbidden configuration in the final state and hence is consistent with the fact that the attractor is the Fibonacci chain.

$m$  and  $n$  respectively, is a *dyad* and is defined as

$$\mathcal{E}_{\alpha_m \beta_n} := \mathbf{E}_{\alpha_m} \otimes \mathbf{E}_{\beta_n} \equiv \mathbf{E}_{\alpha_m} \mathbf{E}_{\beta_n}^T. \quad (13)$$

Unlike in the earlier sections, here the coordinate locations of the individual tiles are referenced from the left (beginning of the chain), eg. the subscript above identifies the location of the  $\alpha$  VC as the  $m^{\text{th}}$  coordinate and so on. The empire matrix  $\mathcal{E}_{\alpha_m \beta_n}$  is a *dyadic product* of two vectors resulting in a tensor of rank two and dimensions  $N \times N$ .

The Hamiltonian operator can be then written as the distributed sum of the symmetrized Empire matrices  $\mathcal{E}_{\alpha_m \beta_n}$  over all possible VCs and location pairs as follows:

$$\mathcal{H} := -\frac{1}{N} \sum_{m,n \in X} \frac{\mathcal{E}_{\alpha_m \beta_n} + (\mathcal{E}_{\alpha_m \beta_n})^T}{2}, \quad (14)$$

where the sum is over all possible pairs of interacting empires of the given chain.  $\mathcal{H}$  is an  $N \times N$  symmetric matrix whose trace gives the Hamiltonian  $H_\Omega$  defined by eq. (12), i.e.  $H_\Omega := \text{Tr}(\mathcal{H})$ . Since the interaction free term of the Hamiltonian prescribed earlier by eq. (12) plays no discernible influence on the evolution of the tiled chain into the Fibonacci configuration, it is omitted from consideration here and only the bilinear interaction terms are retained. Further, the interaction coefficients  $J_{m,n}$  that appear in the eq. (12) are set to unity. Among all possible chain configurations, the Fibonacci chain corresponds to the configuration that minimizes the trace  $H_\Omega = \text{Tr}(\mathcal{H})$  as demonstrated by the Monte Carlo simulations of section 3.2.

#### 4.2 Spectrum of the Hamiltonian $\mathcal{H}$ and theoretical analysis

In this section, we show by spectral analysis of  $\mathcal{H}$  how one may recover the Fibonacci chain if only the collection of all empire configurations associated with a Fibonacci chain of length  $N$  was available (and not the Fibonacci chain itself). After all, the Monte Carlo simulations of section 3 showed that one could find the attractor configuration by relaxing  $H_\Omega$  built entirely of the empires. We will also explain why this Fibonacci attractor corresponds to the ground state of  $\mathcal{H}$  with the highest probability.

$\mathcal{H}$  is a real symmetric matrix and hence has real eigenvalues with  $\lambda_1 = \lambda_{\min} < 0$  corresponding to the ground state energy level  $E_1 \equiv E_{\min}$ . Interestingly, the eigenvector corresponding to  $\lambda_{\min}$  prescribes the distribution of  $L$  and  $S$  tiles of a Fibonacci chain (up to our chosen sign convention). This corroborates the observations made in section 3.2 earlier that the attractor of the chain is the Fibonacci state.

The Hamiltonian  $\mathcal{H}$  can be diagonalized as  $\Psi D \Psi^{-1}$  where the energy eigenvalues are given by the diagonal

coordinate of any chain configuration. Hence, the notion of empires is not restricted to a Fibonacci quasicrystal but applies to any configuration of the chain.

matrix

$$D = \begin{pmatrix} E_1 & 0 & \cdots & 0 \\ 0 & E_2 & \cdots & 0 \\ \cdots & \cdots & \cdots & \cdots \\ 0 & \cdots & \cdots & E_N \end{pmatrix},$$

and  $\Psi$  is a matrix whose columns are the eigenvectors  $\psi_n$  corresponding to the eigenvalues  $E_n$ . By convention,  $|E_1| \geq |E_2| \geq |E_3| \geq \dots$ . In order to obtain the Fibonacci chain exactly in terms of the signed unitary digits,  $-1$  and  $1$  (and not only in their relative distribution of signs), a superposition of the relevant eigenvectors of  $\mathcal{H}$  must be considered. Thus, if one were to posit the Fibonacci state as a quantum state, the Fibonacci state  $\psi_F$  may be written as a linear superposition of  $r + 1$  eigenvectors corresponding to the  $r + 1$  dominant eigenvalues (including the zero eigenvalue) of the matrix  $\mathcal{H}$  whose rank is  $r < N$ , resulting in the following ansatz,

$$\psi_F = \sum_{n \leq r+1} c_n \psi_n, \quad (15)$$

where the  $\psi_n$ s are the orthonormal eigenvectors of  $\mathcal{H}$  and  $\psi_F := \pm \frac{1}{\sqrt{N}} \text{sign } \psi_1$  (see eqs. (17) and (18)). This ansatz is a consequence of the equivalence between the quantum and classical lattice models in the absence of the external field and the fact that the distribution of signs of the entries of  $\psi_1$  prescribes the attractor configuration as explained earlier. The Fibonacci state  $\psi_F$  is degenerate as manifested by the appearance of  $\pm$  in the ansatz because the choice of the labels  $L \rightarrow -1$  and  $S \rightarrow +1$  is arbitrary. Both  $\psi_F$  and  $-\psi_F$  are solutions of  $\mathcal{H}|\psi\rangle = E|\psi\rangle$  [61]. This underscores the fact that it is the relative ordering of the signs of the entries of  $\psi_1$  that essentially dictates the attractor configuration. Further, the matrix  $\mathcal{H}$  is rank deficient because the resulting truncated Fibonacci chain is not an exact quasicrystal but an *approximant* with periodicity equal to  $N$ . Only in the infinite length chain, a full rank matrix Hamiltonian can be obtained. Another interesting observation from Table 1 is that the  $\text{rank}(\mathcal{H})$  for a chain of length  $N$  (corresponding to, say, Fibonacci word  $S_m$ ) is equal to the length of the previous Fibonacci word ( $S_{m-1}$ ) except in some cases where the result is off by one due to numerical imprecision in computing the diagonalization of  $\mathcal{H}$  owing to infinitesimally small numbers involved resulting in roundoff errors. This is likely due to the manner in which the higher Fibonacci words may be generated recursively like  $S_m = S_{m-1} S_{m-2}$ ,  $\forall m \geq 2$  as mentioned earlier in eq. (2).

Table 1:  $rank(\mathcal{H})$  vs  $N$ 

| length of chain, $N$ | $rank(\mathcal{H})$ |
|----------------------|---------------------|
| 5                    | 2                   |
| 8                    | 4                   |
| 13                   | 8                   |
| 21                   | 12                  |
| 34                   | 21                  |
| 55                   | 33                  |
| 89                   | 55                  |
| 144                  | 88                  |
| 233                  | 144                 |

It may be insightful to provide an analogy with quantum mechanical systems. The energy of the Fibonacci state can be obtained as

$$\langle \psi_F | \mathcal{H} | \psi_F \rangle = E_{\psi_F} = \sum_n |c_n|^2 E_n, \quad (16)$$

where  $E_n$  is the  $n^{\text{th}}$  eigenvalue of  $\mathcal{H}$  and denotes the  $n^{\text{th}}$  energy eigenstate and the coefficient  $|c_n|^2$  is the probability of being in state  $\psi_n$ . The latter demands the restriction  $\sum_{n \geq 1} |c_n|^2 = 1$ . It may be interesting to note that if  $|c_n|^2 = \frac{1}{N}$ , then the value of  $E_{\psi_F}$  would be the ensemble average of the energy eigenvalues prescribed by  $H_\Omega$  whence all the energy eigenstates are equally probable, i.e.  $NE_{\psi_F} = \sum_n E_n = Tr(\mathcal{H}) = H_\Omega$ . This equipartition of energy eigenmodes is a signature of the principle of eigenstate thermalization [62, 63, 64]. Further, while the energy eigenstates may be equally probable in occurrence, their magnitudes are distinctly different because  $|E_1| > |E_2| > |E_3| > \dots$  and so on, unless there is a degeneracy of eigenstates. In the present case, as is shown below,  $|E_1| \gg |E_i| \quad \forall i \neq 1$  which guarantees the prominence of the most relevant eigenstate  $\psi_1$ . In the next section, we will discuss if the condition of equiprobable eigenstates, given above, holds or not in the large  $N$  *thermodynamic* limit; and if not, what inference one may draw. In summary, two questions remain central to the inquiry in this paper.

1. How to find the attractor of the Hamiltonian model?
2. Why does the attractor configuration coincide with the Fibonacci chain as demonstrated by the simulations of the previous section?

The answer to the first question is essential to justify the observations of the simulations presented in section 3.2 above. The answer to the second question is important in order to understand the physics of quasicrystal growth and the origin of aperiodicity in physical systems.

#### 4.2.1 How to find the attractor of the Hamiltonian?

Simulations of section 3 prescribe a solution strategy for finding the attractor configuration. Is this attractor solution consistent with our quantum mechanical interpretation of the system? The central idea to find the explicit form of the solution of the final relaxed state of the Hamiltonian (12) is postulated as a superposition of eigenstates (15). Recall the ansatz (15): the attractor configuration is prescribed by sign  $\psi_1$  where  $\psi_1$  is the eigenvector corresponding to the most dominant energy eigenvalue  $E_1$  and sign is the well known signum function. Since the eigenvector corresponding to the most dominant eigenvalue prescribes the distribution of the tiles in the final state up to the chosen sign convention, the exact form of the final Fibonacci state of the chain can be obtained by writing a linear combination of the first  $(r+1)$  eigenvectors with the associated coefficients as mentioned in the expression (15). This will prescribe the correct exact form of the attractor configuration provided

$$\langle \mathbf{c}_{r+1}, \mathbf{c}_{r+1} \rangle = \sum_{i=1}^{r+1} |c_i|^2 = 1,$$

where  $\mathbf{c}_{r+1} = (c_1, c_2, c_3, \dots, c_r, c_{r+1})^T$ . Importantly, this attractor turns out to be the Fibonacci chain of length  $N$ . Figure 4 presents the values of  $\sum_{i=1}^{r+1} |c_i|^2$  for chains of different lengths by considering only the first  $(r+1)$  coefficients. In all cases, the value of  $\sum_{i=1}^{r+1} |c_i|^2$  is very close to unity thereby validating the suitability of eq. (15) to find the exact solution of the final relaxed state of the Hamiltonian. The solution obtained is the Fibonacci chain.

The solution strategy mentioned above is explained here through an example. Consider a chain of length  $N = 13$ . Under similarity transformation,  $\mathcal{H} = \Psi D \Psi^{-1}$  and the rank of  $\mathcal{H}$  is  $r = 8$ . The attractor of this system is obtained by considering the eigenvector

$$\psi_1 = \begin{pmatrix} 0.1962 \\ -0.1962 \\ 0.2917 \\ 0.2403 \\ -0.1941 \\ 0.5313 \\ -0.1455 \\ 0.1455 \\ 0.3860 \\ -0.2452 \\ 0.4366 \\ 0.0954 \\ -0.0954 \end{pmatrix} \quad (17)$$

and using the following ansatz and solving for the coefficients  $c_n$ ,

$$\frac{-1}{\sqrt{13}} \text{sign } \psi_1 = \frac{-1}{\sqrt{13}} \begin{pmatrix} 1 \\ -1 \\ 1 \\ 1 \\ -1 \\ 1 \\ -1 \\ 1 \\ 1 \\ -1 \\ -1 \end{pmatrix} = \sum_{n \leq 8+1} c_n \psi_n. \quad (18)$$

This gives us

$$\mathbf{c}_{r+1} = \begin{pmatrix} c_1 \\ c_2 \\ c_3 \\ c_4 \\ c_5 \\ c_6 \\ c_7 \\ c_8 \\ c_9 \end{pmatrix} = \begin{pmatrix} -0.8873 \\ -0.0335 \\ 0.0107 \\ -0.1524 \\ -0.2994 \\ 0.2110 \\ 0.1909 \\ -0.1328 \\ 0.0000 \end{pmatrix}$$

whence it may be checked that indeed

$$\langle \mathbf{c}_{r+1}, \mathbf{c}_{r+1} \rangle = \sum_{i \leq 8+1} |c_i|^2 = 1.$$

Finally, the attractor configuration  $\psi_F$  is expressed as a superposition of eigenstates (15) by using the coefficients computed above. This solution corresponds to the sixth Fibonacci word  $S_5$  which can be found using the algorithmic recursion  $S_n = S_{n-1}S_{n-2}$ ,  $n \geq 2$ ,  $S_0 = 0, S_1 = 01$ . This paper presents a *physical* model of the emergence of Fibonacci quasicrystal that can also be constructed algorithmically as explained in several papers cited earlier. The solution of  $\mathcal{H}$  is an NP-hard optimization problem that essentially involves finding the most probable ground state energy [61, 65, 66].

#### 4.2.2 Why is the attractor configuration given by the Fibonacci chain?

While the ansatz allows us to find the attractor solution consistent with the postulates of quantum mechanics, a natural question that follows is: *why is the attractor configuration given by the Fibonacci chain?* After all, shouldn't one expect the relaxation of the Hamiltonian resemble thermalization resulting in equipartition of energy among the different eigenstates? In fact, to the contrary, eigenstate thermalization would imply the absence of an attractor solution as multiple final states would be equally probable. So if one is looking for an attractor as a solution,

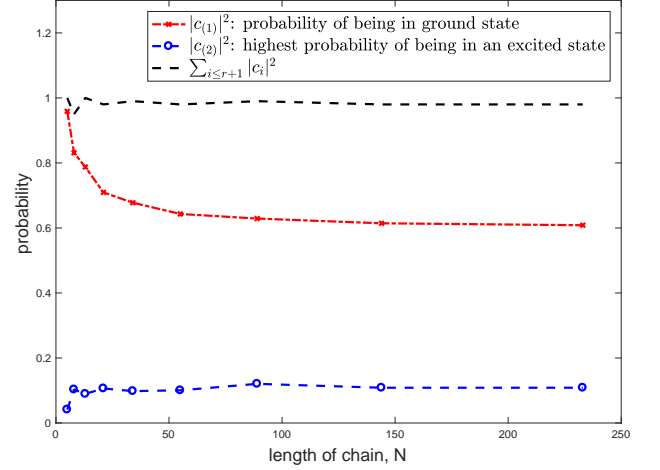


Fig. 4: This plot shows that the probability of the Fibonacci state being the ground state is significantly higher than being in any other excited state. Further, it is shown that the solution prescribed by eq. (15) is consistent with the fundamental axiom of probability,  $\sum_{i \leq r+1} |c_i|^2 = 1$ .

and consequently a model of quasicrystal growth, thermalization is undesirable. So it works to our advantage that the Hamiltonian  $\mathcal{H}$  does not thermalize to equiprobable eigenstates.

In fact, let us rewrite the spectral decomposition given by eq. (16) as

$$E_{\psi_F} = \sum_n |c_n|^2 E_n = \sum_{(m)} |c_{(m)}|^2 E_{(m)}, \quad (19)$$

where by convention  $|c_{(1)}|^2 \geq |c_{(2)}|^2 \geq |c_{(3)}|^2 \geq \dots$  and  $E_{(m)} \in \rho(\mathcal{H})$  (spectrum of  $\mathcal{H}$ ) is such that its coefficient is  $c_{(m)}$ . In other words, the second equality is simply a re-arrangement of the summands in  $\sum_n |c_n|^2 E_n$  that obeys the above inequalities and sorts the energy eigenstates in decreasing order of the probability of finding the Fibonacci chain in that state. It turns out that  $c_{(1)} \equiv c_1$  and consequently  $E_{(1)} \equiv E_1$ . More importantly, the Hamiltonian  $\mathcal{H}$  is such that  $|c_{(1)}|^2 \gg |c_{(2)}|^2$  as shown clearly in Figure 4. In section 3, we have presented results of numerical experiments that established that of all the possible configurations, it is the Fibonacci configuration that minimizes the

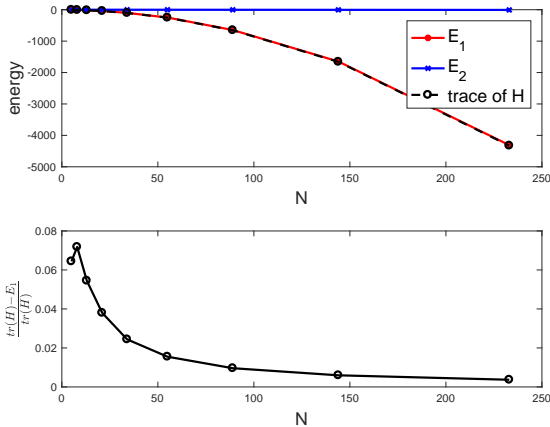


Fig. 5: Top: Energy eigen values  $E_1$  and  $E_2$  of the hamiltonian  $\mathcal{H}$  are plotted along with the trace of the Hamiltonian which gives the total energy of the system. Clearly,  $|E_1| \gg |E_2|$ . Bottom: This plot shows that the relative error in the approximation of  $\text{Tr}(\mathcal{H})$  by  $E_1$  decreases as  $N$  increases and is practically miniscule. The plots show that for moderately large  $N$ ,  $\text{Tr}(\mathcal{H})$  can be well approximated by  $E_1$ .

total Hamiltonian  $H_\Omega = \text{Tr}(\mathcal{H})$ . Note that practically almost all of the total energy of the system is concentrated in the ground state as illustrated by Figure 5. In essence, since  $E_1 \rightarrow H_\Omega$  as  $N$  becomes large enough, it follows that the Fibonacci configuration not only minimizes  $H_\Omega$  among all possible chain configurations but also minimizes the ground state energy among all possible chain configurations. This establishes that the Fibonacci chain is the *most probable* ground state of the Hamiltonian  $\mathcal{H}$  and by a big margin (see Figure 4).

It must be emphasized here that the ability of the empires, through simple non-local interactions as prescribed by the r.h.s. of eqs. (12) and (14), to form the final Fibonacci state of the chain renders the empires as the generators of the Fibonacci chain and fundamental elements in a model of aperiodic order. It can be shown that the simple nearest neighbor Ising model does not generate the Fibonacci chain.<sup>6</sup> Essentially, it is the *non-local* scope of

the empires that is the quintessential element in modeling quasicrystal growth. This inherent non-local aspect of the model permits a quantum mechanical analogy.

### 4.3 Symmetries and comparison with the Ising model

The most fundamental symmetry in crystalline structures is translation symmetry. This symmetry is absent in quasicrystalline structures. In the current case under investigation here, the precise algebraic form in which a translation asymmetry pertaining to the Fibonacci quasicrystal may be conceptualized is illustrated by eqs. (9), (10) and (11). These empires collectively characterize all forbidden configurations of the Fibonacci chain. The Hamiltonian  $\mathcal{H}$  encodes the exact physical mechanism which manifests this translation asymmetry through the interaction of the empires.

Of course, this beckons a natural comparison with other lattice models especially with the most widely-known nearest neighbor Ising Hamiltonian. At the outset, it must be clarified that the Monte Carlo simulation of the nearest neighbor Ising Hamiltonian, that relies entirely on local spin-spin interactions, does not generate the Fibonacci chain or any one dimensional quasicrystal. This clearly underscores the necessary role of non-local interactions in a model of quasicrystal growth.

The definition of the empires (as illustrated by the examples (5) and (6), and the top and bottom figures on the left panel of Figure 3) imply that the inner product  $J_{m,n} \langle \mathbf{E}_{\alpha_m} | \mathbf{E}_{\alpha_n} \rangle$  in eq. (12) is essentially equivalent to  $\sum_{i=1}^N J_{m,n}^i s_i^m s_i^n = \sum_{i=1}^N J_{m,n}^i s_i^2$  because  $s_i^m = s_i^n = s_i$  where  $s_i$  labels the  $i^{\text{th}}$  tile of the chain under consideration. Hence, one may attempt to devise an equivalent zero-field lattice model of the form

$$\begin{aligned} H_\Omega^{(1)} &= -\frac{1}{N} \sum_{m,n \in X} \sum_{i=1}^N J_{m,n}^i s_i^m s_i^n \\ &= -\frac{1}{N} \sum_{m,n \in X} \sum_{i=1}^N J_{m,n}^i s_i s_i \\ &= -\frac{1}{N} \sum_{m,n \in X} \sum_{i=1}^N J_{m,n}^i s_i^2 \end{aligned} \quad (20)$$

that generates the Fibonacci chain. Here  $s_i = \pm 1$  and  $\mathbf{J}_{m,n} \equiv J_{m,n}^i$  is a vector for every  $m$  and  $n$  with non-zero unit entries at locations where the effect of the spins ( $s_i^2$ ) must be accounted for. In this sense,  $J_{m,n}^i$  are *non-local* coupling constants indexed by  $i$  and the vectors themselves are labelled by the  $m$  and  $n$  lattice sites. A careful observation of the interaction terms in the Hamiltonian (12) and the definition of the empire vectors reveals the formal similarities with the Hamiltonian (20). However, such an attempt to engineer the coupling constants does not encode the information of the projection from a higher dimensional space. Moreover, there does not appear a simple way to construct the coupling constants

<sup>6</sup> [https://www.youtube.com/watch?v=N85\\_add\\_1UI](https://www.youtube.com/watch?v=N85_add_1UI)

$J_{m,n}^i$  and hence using model (20) to perform the analysis and the simulations, instead of the equivalent models (12) and (14), would be very challenging. On the other hand, the empires provide us with a tool to model non-local interactions very naturally and share a geometrical significance as the generators of the Fibonacci chain because they are derived by projection from a higher dimension which has translation symmetry. In any case the model (12) presented here is clearly *not* an Ising model for reasons mentioned above.

Like the nearest neighbor Ising model, the Hamiltonian  $H_\Omega$  is invariant under spin inversion as mentioned earlier. This is so because the inner product between the empire vectors is invariant under spin inversion. Eg., consider  $\mathbf{E}_{\alpha_m} = (s_1 s_2 s_3 \dots s_N)$  and  $\mathbf{E}_{\beta_n} = (s'_1 s'_2 s'_3 \dots s'_N)$  where  $s_i, s'_i = -1, 1$  or  $0$  depending on  $x_i = L, S$  or if it is an unforced tile. Clearly, the spin inversion  $s_i \rightarrow -s_i$  and  $s'_i \rightarrow -s'_i$ , which is essentially flipping the labels of  $L$  and  $S$ , preserves  $\langle \mathbf{E}_{\alpha_m} | \mathbf{E}_{\beta_n} \rangle$ .

However, unlike the zero external field nearest neighbor Ising model in one-dimension or the nearest neighbor Ising model in a square lattice in two-dimensions, the zero-external field ( $B_{\alpha_k, i} \equiv 0$ ) partition function  $Z_\Omega = Tr(e^{-\beta H_\Omega})$  based on eq. (12), and thereby the free energy density, are not invariant under sign inversion of the coupling coefficients  $J_{j,i}$ . This is because the non-zero entries of the interacting empire vectors change sign concurrently. This is further illustrated by the equivalent model (20). Therefore, the thermodynamic properties of the model presented here are not the same under the reversal of sign of the coupling constants  $J_{j,i}$ .

## 5 Summary of main results

The main novel contributions of this paper are summarized below.

1. Algebraic forms of the empires of the VCs of a Fibonacci chain are provided for the first time to our knowledge. The closed form expressions are verified in agreement with earlier known methods of computing empires of VCs using geometric and algorithmic methods. These algebraic forms enable us to know the exact manner by which the translation symmetry is absent in a Fibonacci chain.
2. A Hamiltonian is constructed using the empires mentioned above and Monte Carlo simulations are performed. The simulations show that the Fibonacci chain is an attractor of the model.
3. The Hamiltonian is promoted to a matrix operator form and a spectral analysis is performed to find the relevant eigenstates. An ansatz is provided to find the attractor configuration analytically. It is verified to be true and consistent for a chain of any finite length. A quantum mechanical interpretation reveals that the Fibonacci chain is the most probable ground state of the system and hence provides a theoretical explanation of the attractor configuration. The theoretical analysis shows that the Fibonacci configuration not only

minimizes the total Hamiltonian (total energy) of the system but also minimizes the ground state of the system.

4. The paper presents a new physically realizable model of quasicrystal growth based on non-local interactions. To our best knowledge, this may be the first Hamiltonian based lattice model whose ground state is the Fibonacci quasicrystal.

## 6 Future research directions

Two immediate research directions follow naturally from the model analyzed here. Firstly, there seems a formative correspondence between the empire Hamiltonian presented in this paper and the well known spin-1 Ising model owing to the use of ternary elements. Secondly, the one-dimensional model described here may be extended to a two dimensional model of quasicrystal growth by relaxing a network of chains (fibers). These directions are discussed briefly below.

### 6.1 Spin 1 lattice model and angular momentum operators

The empire vectors of eqs. (12) and (13) that define the Hamiltonian  $H_\Omega$  and  $\mathcal{H}$  are made of ternary elements  $\{1, -1, 0\}$ . This suggests a correspondence with the spin-1 Ising model associated with the spin-1 angular momentum matrices  $L^x, L^y, L^z$ , each of dimension  $3 \times 3$  [67, 68]. The diagonal entries of  $L^z$  are  $1, 0$  and  $-1$ . The key difference in our case with respect to the spin-1 Ising model is that the empire vectors have a non-local scope and the Hamiltonian implements non-local interactions  $\langle \mathbf{E}_{\alpha_m} | \mathbf{E}_{\beta_n} \rangle$  between the  $m^{\text{th}}$  and  $n^{\text{th}}$  lattice sites. Furthermore, since the number of vertex types  $\alpha, \beta = 1, 2, 3$  also matches the number of spatial directions  $x, y, z$ , one may propose the following zero-field Hamiltonian

$$\mathcal{H}^{(2)} = - \sum_{a=\{x,y,z\}} \sum_{m,n \in X} J_{m,n} \mathcal{L}_m^a \mathcal{L}_n^a \quad (21)$$

as a *non-local* generalization of the spin-1 nearest neighbor Hamiltonian. Here,  $a, b = 1, 2, 3$  correspond to  $x, y, z$  and  $J_{m,n}$  are the non-local coupling constants between lattice sites  $m$  and  $n$ . By defining,  $\mathcal{L}_m^a := I^{\otimes m-1} \otimes L^a \otimes I^{\otimes N-m}$ ,  $a = x, y, z$ , as  $3^N \times 3^N$  matrices and appropriately engineering  $J_{m,n}$ , we propose to investigate if there is any correspondence between  $\mathcal{H}^{(2)}$  stated above by eq. (21) and the Hamiltonian of eq. (14). It may be interesting to note that the model (21) is similar in spirit to a non-local version of the Heisenberg model [20, 59] that has shown promise in the study of ferrimagnetic effects [69, 70, 71, 72] and for investigating quantum spins in quasiperiodic anti-ferromagnets [73]. Further, unlike the spin-1 Ising model, it may be interesting to allow for cross-interactions in the form of  $\mathcal{L}_m^x \mathcal{L}_n^y$  etc. and investigate the behavior of the model. It must be stated that appropriately engineering the coupling constants  $J_{m,n}$  will present a formidable challenge.

## 6.2 Network of Fibonacci chains in 2D

We will extend the formalism to a tiling network in two dimensions with overall pentagonal symmetry as an example.

**Tiling matrix T:** The tiling space is a network of 2-alphabet chains with a suitable matrix representation denoted by  $T_{i,k_i}^{j,k_j}$  where  $i, j \in \{1, 2, 3, 4, 5\}$  denote the chain species and  $k_i, k_j$  index the entries from the respective chain species and take on values between  $-N$  and  $N$ . Thus we have  $2N + 1$  members in each species. To account for 5-fold symmetry, we have five distinct chain species. The reader is referred to Figure 6. This formalism can be easily extended to any general  $n$ -fold symmetry by having  $n$  chain species.

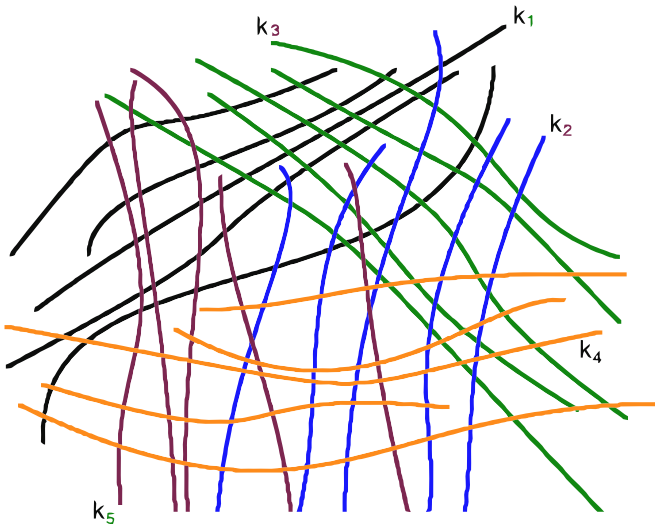


Fig. 6: Topological representation of the tiling network where each chain species is shown with a different color. The  $k_i$  for each chain species indexes the corresponding member of that species and takes on values between  $-N$  and  $N$ . Each member of every chain species has a unique  $k_i$  index. Note that the graphic is only partially displayed and that the chains of each species are longer than shown here as each of them intersect with every member of all other species.

The entries of the matrix  $T$  are  $-1, 1$  or  $0$  as in the 1D case, where  $0$  represents absence of a tile. The entries of the  $T$  matrix represent the tile type associated at the intersection of lines  $k_i$  and  $k_j$ . Moreover, the network topology prohibits the intersection of three or more lines at the same site. Member chains of the same species never intersect with each other. There are no loops. The matrix  $T$  is symmetric in its upper and lower arguments. Math-

ematically, the above constraints can be enumerated as follows,

1.  $T_{i,n}^{i,m} = 0, \quad m \neq n,$
2.  $T_{i,n}^{j,m} = T_{j,m}^{i,n}.$

The network of chains mentioned above will be relaxed using a Monte Carlo simulation under the constraints listed above and the attractor configuration will be investigated corresponding to the minimum of the total Hamiltonian. We conjecture that the relaxed state will correspond to the Penrose tiling which is a two dimensional quasicrystal. Thus we can put this framework to test as a generalized model of quasicrystal growth in two dimensions. Subsequently, the model will be extended to three dimensions. Such topological order with inherent quasicrystalline structure has been studied recently based on a quantum string-net Hamiltonian [74]. Simulations of interacting Fibonacci anyons, with relevance in quantum computing technology, have been analyzed using tensor network approaches [75] which further emphasizes the importance of research on the proposed topic.

## Acknowledgments

The first author wishes to acknowledge some useful discussions with Raymond Aschheim regarding empires of vertex configurations. The second author wishes to thank Meredith Bowers for her support. The authors would also like to acknowledge the generous hospitality of Mr. Narendra Sharma and his team of Thapar Institute for making the stay of the second author a very pleasant experience.

## Authors contributions

Both authors were involved in the development of the model and in the preparation of the manuscript. Both authors have read and approved the final manuscript.

## References

- [1] M. Senechal. *Quasicrystals and Geometry*. Cambridge University Press, 1995.
- [2] M. Baake and U. Grimm. *Aperiodic Order: Volume 1, A Mathematical Invitation*. Cambridge University Press, 2013.
- [3] C. Janot. *Quasicrystals - A Primer*. Oxford University Press, 1994.
- [4] S. Ostlund and P. J. Steinhardt. *The Physics of Quasicrystals*. World Scientific Publishing Co., 1987.
- [5] D. J. Gross. In: *Proc. Natl. Acad. Sci. USA* 93 (1996), p. 14256.
- [6] K. Brading and E. Castellani. *Symmetries in Physics: Philosophical Reflections*. Cambridge University Press, 2003.
- [7] H. Genz. In: *Interdisciplinary Science Reviews* 24 (1999), p. 129.

- [8] R. Lifshitz. In: *Isr. J. Chem.* 51 (2011), p. 1156.
- [9] P. Steinhardt. In: *NATURE* 452 (6) (2008), pp. 43–44.
- [10] A. Sen, R. Aschheim, and K. Irwin. In: *Mathematics* 5 (29) (2017).
- [11] W. Steurer. In: *Z. Anorg. Allg. Chem* 637 (2011), p. 1943.
- [12] H. C. Jeong. In: *Phys. Rev. Letts.* 98 (2007), p. 135501.
- [13] U. Gaenshirt and M. Willsch. In: *Philosophical Magazine* 87 (2007), p. 3055.
- [14] A. Haji-Akbari. In: *Nature Letters* 462 (10) (2009).
- [15] A. Katz and M. Duneau. In: *Scripta Metallurgica* 20 (1986), p. 1211.
- [16] I. Blinov. In: *Scientific Reports* 5 (2015), p. 11492.
- [17] P. Vignolo et al. In: *Phys. Rev. B* 93 (2016), p. 075141.
- [18] M. Engel et al. In: *Nature Materials* (2014), p. 4152.
- [19] A. Kiselev, M. Engel, and H. R. Trebin. In: *Phys. Rev. Letts.* 109 (2012), p. 225502.
- [20] N. Goldenfeld. *Lectures on phase transitions and the renormalization group*. Levant Books, 2005.
- [21] P. Lounesto. *Clifford Algebra and Spinors*. Cambridge University Press, 2001.
- [22] T. Janssen, O. Radulescu, and A. Rubtsov. In: *Eur. Phys. J. B* 29 (2002), pp. 85–95.
- [23] M. de Boissieu, R. Currat, and S. Francoual. In: *Handbook of Metal Physics*. Vol. 3. Elsevier, 2008. Chap. 5: Quasicrystals: Phason modes in aperiodic crystals, pp. 107–169.
- [24] M. Widom. In: *Philosophical Magazine* 188 (2008), p. 13.
- [25] M. de Boissieu. In: *Acta Cryst.* A75 (2019), p. 273.
- [26] T. Janssen, G. Chapuis, and M. de Boissieu. In: *IUCr Monographs on Crystallography*. 1st. Vol. 3. Oxford University Press, 2007. Chap. Aperiodic Crystals. From Modulated Phases to Quasicrystals: Structures and Properties, pp. 107–169.
- [27] R. Currat and T. Janssen. In: *Solid State Physics*. Ed. by H. Ehrenreich and D. Turnbull. 1st. Vol. 41. Elsevier, 1988. Chap. Excitations in Incommensurate Crystal Phases, pp. 201–302.
- [28] M. Engel, S. Sonntag, and H. Trebin. In: *Phys. Rev. B* 81 (2010), p. 064302.
- [29] J. A. Kromer et al. In: *Eur. Phys. J. E* 36 (2013), p. 25.
- [30] M. Engel et al. In: *Phys. Rev. B* 75 (2007), p. 144203.
- [31] V. I. Zubov and J. N. Texeira Rabelo. In: *Phys. Rev. B* 49 (1994), p. 8671.
- [32] L. D. Gronlund, D. C. Wright, and J. P. Sethna. In: *Phys. Rev. B* 42 (1990), p. 8517.
- [33] P. Bak and J. von Boehm. In: *Phys. Rev. B* 21 (1980), p. 5297.
- [34] W. N. Yessen. In: *Annales Henri Poincaré* 15 (2014), p. 793.
- [35] T. Dotera. In: *Materials Science Forum*. Ed. by K. H. Kuo and S. Takeuchi. Vol. 150-151. Scientific.Net, 1994. Chap. Phason Elasticity and Ising Models, pp. 201–302.
- [36] S. Ostlund et al. In: *Phys. Rev. Letts.* 50 (23) (1983), p. 1873.
- [37] K. Giergiel, A. Kuroś, and K. Sacha. In: *Phys. Rev. B* 99 (2019), 220303 (R).
- [38] V. Wiggers and P. C. Rech. In: *Eur. Phys. J. B* 91 (144) (2012), pp. 1–6.
- [39] Y. Achiam, T. C. Lubensky, and E. W. Marshall. In: *Phys. Rev. B* 33 (9) (1986), p. 6460.
- [40] H. Tsunetsugu and K. Ueda. In: *Phys. Rev. B* 36 (1987), p. 5493.
- [41] A. Mookerjee and V. A. Singh. In: *Phys. Rev. B* 34 (10) (1986), 7433 (R).
- [42] N. Macé, A. Jagannathan, and F. Piéchon. In: *Phys. Rev. B* 93 (20) (2016), 205153:1–11.
- [43] J. Bellissard et al. In: *Commun. Math. Phys.* 125 (1989), pp. 527–543.
- [44] D. Tanese et al. In: *Phys. Rev. Letts.* 112 (2014), 146404:1–5.
- [45] A. Ghosh and S.N. Karmakar. In: *Eur. Phys. J. B* 11 (1999), pp. 575–582.
- [46] A. Mukherjee, A. Nandy, and A. Chakrabarti. In: *Eur. Phys. J. B* 90 (2017), pp. 52–59.
- [47] C. Castro. In: *Chaos, Solitons and Fractals* 14 (2002), p. 1341.
- [48] W. Chuan. In: *Fibonacci Quaterly* 33 (1995).
- [49] W. Chuan. In: *Applications of Fibonacci Numbers*. Ed. by G. E. Bergum, A. N. Philippou, and A. F. Horadam. Springer, Dordrecht, 1996. Chap. Subwords of the Golden Sequence and the Fibonacci Words.
- [50] N. G. de Bruijn. In: *Indagationes Mathematicae* 43 (1981), p. 39.
- [51] B. Grunbaum and G.C. Shephard. *Tilings and Patterns*. Dover Books on Mathematics, 1987.
- [52] A. Carbone, M. Gromov, and P. Prusinkiewicz. *Pattern Formation in Biology, Vision and Dynamics*. World Scientific Publishing, 2000.
- [53] M. Gardner. *Penrose Tiles to Trapdoor Ciphers: And the Return of Dr Matrix (Spectrum)*. W H Freeman, NY, 1989.
- [54] L. Minnick. Honors thesis. Williams College, 1998.
- [55] J. B. Healy. Honors thesis. Williams College, 2000.
- [56] L. Effinger-Dean. Honors thesis. Williams College, 2006.
- [57] D. Hammock, F. Fang, and K. Irwin. In: *Crystals* 8 (2018), p. 370.
- [58] F. Fang, D. Hammock, and K. Irwin. In: *Crystals* (2017), p. 225911.
- [59] R. J. Baxter. *Exactly Solved Models in Statistical Mechanics*. Academic Press, London, 1982.
- [60] P. Fendley. “Modern Statistical Mechanics”. Book in preparation (<http://users.ox.ac.uk/~phys1116/>). 2019.
- [61] A. Lucas. In: *frontiers in PHYSICS* 2 (2014), pp. 1–15.
- [62] M. Srednicki. In: *Phys. Rev. E* 50 (1994), p. 888.
- [63] M. Rigol, V. Dunjko, and M. Olshanii. In: *Nature* 452 (2009), p. 854.
- [64] M. Rigol and M. Srednicki. In: *Phys. Rev. Letts.* 108 (2012), p. 110601.

- [65] Z. Bian et al. In: *frontiers in PHYSICS* 2 (2014), pp. 1–10.
- [66] N. De La Espriella, G. M. Buendia, and J. C. Madera. In: *Journal of Physics Communications* 2 (2018), p. 025006.
- [67] J. Oitmaa and A. M. A. von Brasch. In: *Phys. Rev. E* 67 (2003), p. 172402.
- [68] T. Kaneyoshi. In: *Journal of the Physical Society of Japan* 56 (1987), p. 933.
- [69] T. Shimokawa and H. Nakano. In: *J. Phys. Soc. Jpn.* 81 (2012), p. 084710.
- [70] G. S. Tian. In: *Phys. Rev. B* 56 (1997), p. 5355.
- [71] J. Rossler and D. Mainemer. In: *Condensed Matter Physics* 13 (1) (2010), 13704: 1-8.
- [72] J. Girovsky et al. In: *Nature Communications* 8 (2017), p. 15388.
- [73] A. Jagannathan. In: *Eur. Phys. J. B* 85 (68) (2012), pp. 1–20.
- [74] P. Fendley, S. V. Isakov, and M. Troyer. In: *Phys. Rev. Letts.* 110 (2013), p. 260408.
- [75] R. N. C. Pfeifer et al. In: *Phys. Rev. B* 82 (2010), p. 115126.